AMBIGUITY FUNCTIONS, WIDE BAND AND NARROW BAND APPROXIMATIONS, AND HIGH DUTY CYCLE SONARS

Paul C. Hines[a],   Stefan M. Murphy[a], Jeffrey R. Bates[b],   Matthew Coffin[c]

[a]Dept. Electrical and Computer Eng., Dalhousie University, PO Box 15000, Halifax NS
[b]Science and Technology Organization - Centre for Maritime Research and Experimentation, La Spezia, SP, ITALY
[c]GeoSpectrum Tehnologies Inc., Dartmouth, NS, Canada, B3B 1J4

contact: Dr. Paul C. Hines, Electrical and Computer Eng., Dalhousie University, PO Box 15000, Halifax NS, B3H 4R2, email: phines50@gmail.com

Abstract: *There is considerable interest in using high duty cycle (HDC) waveforms in modern active sonars. Furthermore, the increase in signal energy that results from using HDC pulses enables wider frequency bandwidths to be transmitted, since there is a reduced requirement to use a high-Q transducer to maximize energy. The combination of high duty cycle and wide frequency band can lead to very large time-bandwidth (TB) products. Although this can provide high coherent gains out of the matched filter, it can also lead to systems that are hypersensitive to both Doppler and range accuracy. Since many sonar performance models employ approximations, it seems germane to examine the validity of some common approximations in the context of these pulses, and to compare the results to theory. The theoretical work is complemented with measurements taken during the Littoral Continuous Active Sonar (LCAS) Multi-National Joint Research Project (MN-JRP) off the coast of La Spezia Italy in October of 2015.*

Keywords: *Channel coherence, high duty cycle (HDC) sonar, matched-filter processing, Doppler spreading, time spreading*

1. INTRODUCTION

There is considerable interest in employing high duty cycle (HDC) waveforms in modern active sonars. In addition to using longer duration pulses, the pulse bandwidths are often increased in HDC sonars. This is possible because the long-duration pulses reduce the requirement to use a high-Q transducer to maximize energy output. However, the resulting increase in the time-bandwidth (*TB*) can fall well outside the region of validity of common sonar approximations such as the narrowband and wideband approximation [1]. In this paper some numerical examples are examined and compared to theory and experiment. The pulses chosen for the comparison were used during LCAS15; each had a bandwidth of 800 Hz and durations of 1 second (PAS) and 20 seconds (HDC), providing *TB* values of 800 and 16000, respectively.

This paper will begin by briefly reviewing how *TB* affects the output of the matched filter with particular emphasis on Doppler and time-spreading sensitivity. Then an experiment done during the LCAS15 will be described. Finally some theoretical results will be compared to the experimental data.

2. THE NARROWBAND AND WIDEBAND APPROXIMATIONS

The narrowband approximation employed in radar and sonar assumes that the effect of a constant Doppler target on the matched-filter output can be represented by a simple frequency translation of the transmitted signal; however, this ignores the compression or dilation of the time (or range) axis. As described in [2], the narrow band approximation estimates the Doppler tolerance based on the temporal overlap loss, whereas the actual tolerance must also account for the mismatch of the slope. It is the latter mismatch that dominates correlation loss in high *TB* waveforms. The wideband approximation derived in [2] states that for a linear LFM pulse, the one-way Doppler velocity tolerance allowed before a 3 dB loss in correlation occurs, is approximated by:

$$V_{wb} = 2600/(B \times T), \tag{1}$$

for bandwidth *B* in Hz, and pulse duration *T* in s, and V_{wb} is measured in m/s. The narrowband approximation states that the one-way Doppler velocity mismatch at which a 3 dB loss in correlation occurs for a linear FM pulse, is approximated by

$$V_{nb} = 435 \times B/f_o, \tag{2}$$

for bandwidth *B*, and center frequency, *fo*, both given in Hz, and V_{nb} is measured in m/s. A useful rule of thumb is provided by Nielsen [1] in which he states that if $V_{wb} < V_{nb}$ then the narrowband approximation is no longer valid and one must resort to the wideband approximation. Table 1 compares the approximations for the LCAS LFM waveforms. In all cases $V_{wb} \ll V_{nb}$ and the narrowband approximation should not be used.

Pulse	f_o (Hz)	Bandwidth (Hz)	Duration (s)	V_{nb} (m/s)	V_{wb} (m/s)
HDC$_{low}$	2200	800	20	158	0.16
HDC$_{high}$	3100	800	20	112	0.16
PAS$_{high}$	3100	800	1	112	3.3

Table 1: Comparison of Doppler velocity tolerance for LFM HDC and PAS pulses from LCAS15.

3. THE LFM AMBIGUITY FUNCTION AND WIDEBAND APPROXIMATION

Although the approximations highlighted in the previous section are useful, more insight can be gained by examining the wideband approximation in the context of the ambiguity function (AF) diagram for an LFM pulse. Kramer [2] expresses the envelope of the complex cross-correlation Doppler channel response, $|R|$, in terms of Fresnel integrals:

$$|R| = \frac{1}{2U} \sqrt{\left[C\left(\frac{A}{U} + U\right) - C\left(\frac{A}{U} - U\right)\right]^2 + \left[S\left(\frac{A}{U} + U\right) - S\left(\frac{A}{U} - U\right)\right]^2} \tag{3}$$

where S and C are the Fresnel sine and cosine integrals, respectively. The variables U and A are given by

$$U = \sqrt{|\Delta v/c|TB\left(1 - \frac{\Delta v/c}{2}\right)} \cong \sqrt{|\Delta v/c|TB} \tag{4}$$

and

$$A = f_o T \Delta v/c - B\Delta t \tag{5}$$

c is the acoustic wave speed and Δv, Δt are the Doppler and time mismatches, respectively. The AF for the HDC and PAS pulse for a center frequency of 3100 Hz is plotted in Fig. 1 as a function of Doppler and time mismatch using parameters contained in Table 1. (Note that plotting the AF in terms of normalized Doppler ($f_o T \Delta v/c$) and time ($B\Delta t$) would result in identical plots for HDC and PAS.) Setting $A = 0$ in (3) obtains:

$$|\hat{R}| = \frac{1}{U} \sqrt{[C(U)]^2 + [S(U)]^2} \tag{6}$$

which corresponds to the ridge line (peak) of the ambiguity function [2]. Plotting (6) as a function of U shows the decorrelation of the matched filter as one moves along the ridge line. (See the *lhs* of Fig. 2). Defining the Doppler tolerance as the value $|\hat{R}|^2 = 0.5$ returns a value of $U \approx 1.32$. Substituting this value for U into (4) and assuming an acoustic wave speed of 1500 m/s results in the wideband approximation in (1). Equation (1) is plotted as a function of TB on a log-log scale in the *rhs* of Fig. 2. The two points on the line
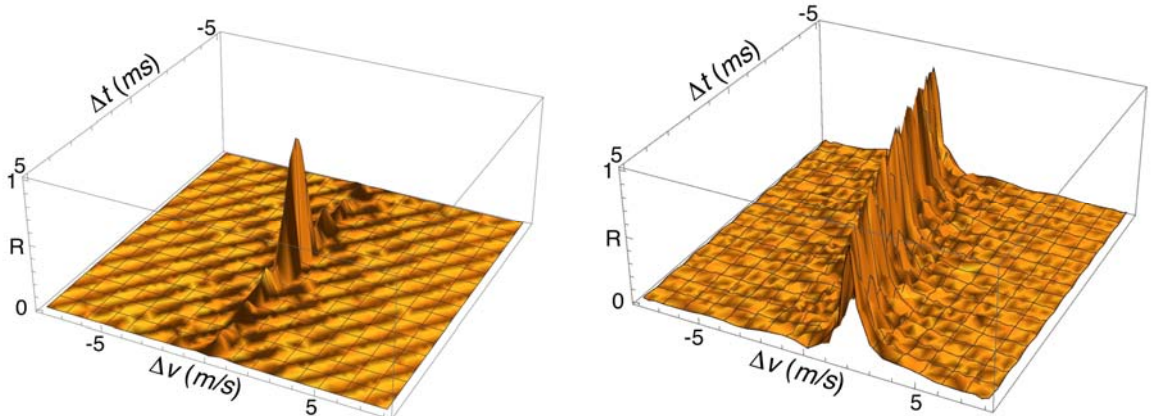

Fig. 1: Ambiguity diagram for HDC*high* pulse (left) and PAS*high* pulse (right) for LCAS LFM parameters plotted verses mismatch in Doppler (m/s) and time (ms). (See Table I for pulse parameters).

represent the PAS (3.3 m/s) and HDC (0.16 m/s) values in Table I. While the parameters of both the PAS and HDC pulses require application of the wide band approximation, it is

only the much larger *TB* of the HDC pulse that results in substantial Doppler sensitivity. This will be demonstrated in the next section using data from LCAS15.
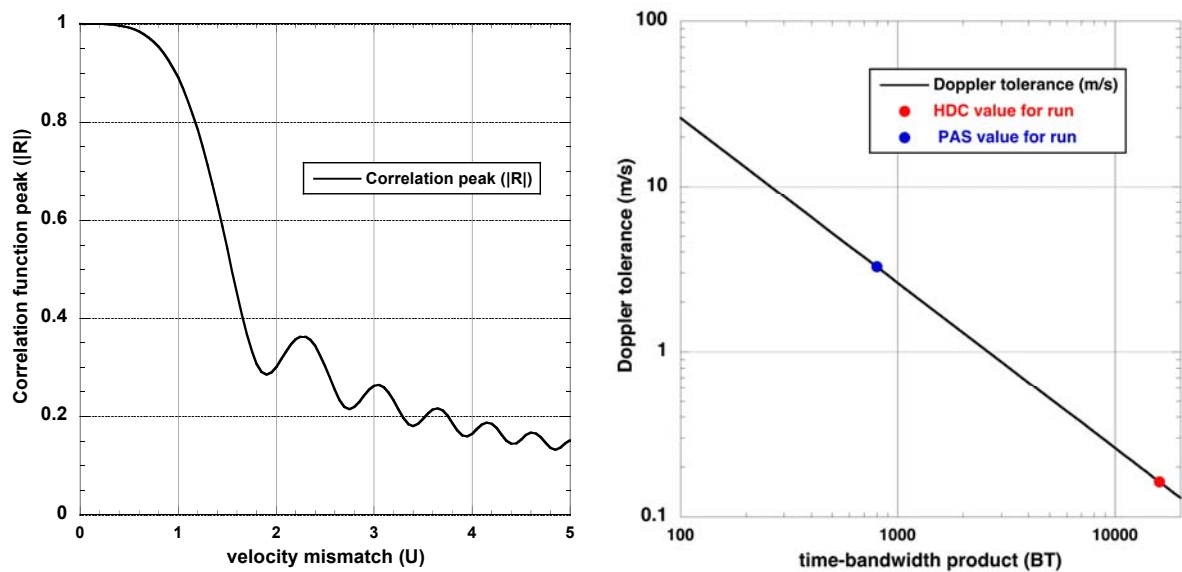

Fig. 2: LHS: Correlation envelope from Equations 6. RHS: Doppler tolerance from Equation 1 highlighting the tolerance of the PAS (blue point) and HDC (red point) pulses used in the experiment.

4. EXPERIMENTAL RESULTS

A full review of the LCAS15 experiment is outside the scope of this short paper so we shall focus on a specific run to contrast the matched-filter results for an HDC and PAS pulse of a fixed bandwidth. LCAS15 was conducted in approximately 100 m of water just off the Italian coast, near La Spezia. A hydrophone was moored on the 110 m contour, at a depth of about 78 m. *RV* Alliance commenced the run at a range of about 10 km northwest of the hydrophone mooring on the 110 m contour, closed on the mooring at a speed of about 2 m/s, turned and opened from the mooring to a range of about 11 km. HDC and PAS signals were transmitted every 20 seconds with the start of both pulses aligned in time. The CPA was about 1 km and occurred twice during the run—at ping 280 as the ship passed the mooring on the closing run, and again at ping 385 as it passed it on the opening run. The pulses were transmitted in adjacent frequency bands, with the HDC centered on 2200 Hz and the PAS centered on 3100 Hz. A 100 Hz guard band from 2600–2700 Hz separated the two bands. (Note that a run was also done with HDC pulses transmitted in both bands to ensure that the HDC-PAS comparison was not significantly affected by the frequency offset of the two pulses. Although data from that run are not included in the paper, the results did indicate that the differences in the HDC and PAS results were not greatly affected by the difference of the HDC-PAS center frequency.) The source was CMRE's mid-frequency, free-flooding ring (Atlas) array and was towed at a depth of 45 m. The amplitude of the input signal was shaped to remove any frequency dependence in the transmitter voltage response of the source. Equal energy was transmitted in both pulses by scaling the relative amplitudes of the PAS and HDC signals by $\sqrt{T_H/T_P}$, where T_H, T_P are the pulse durations of the HDC and PAS.

The matched-filter output of the HDC and PAS signal at the hydrophone is shown for the entire run in Fig. 3. The first thing to note is that although there are signal-level variations during the run between HDC and PAS, the mean levels across the entire run are within 0.5 dB of one another (HDC = 91.4 dB, PAS=91.7 dB). It is somewhat surprising

that the much longer duration of the HDC pulse didn't lead to greater coherence loss. This may be due to the strongly downward refracting sound-speed profile during the run which reduced surface interactions of the signals. To examine the Doppler sensitivity, the data were processed with a set of replicas ranging from about -6 m/s – +6 m/s with a resolution of 0.05 m/s for PAS (241 replicas) and 0.025 for HDC (481 replicas). Each datum point in the figure represents the maximum amplitude arrival in time and Doppler for that ping.
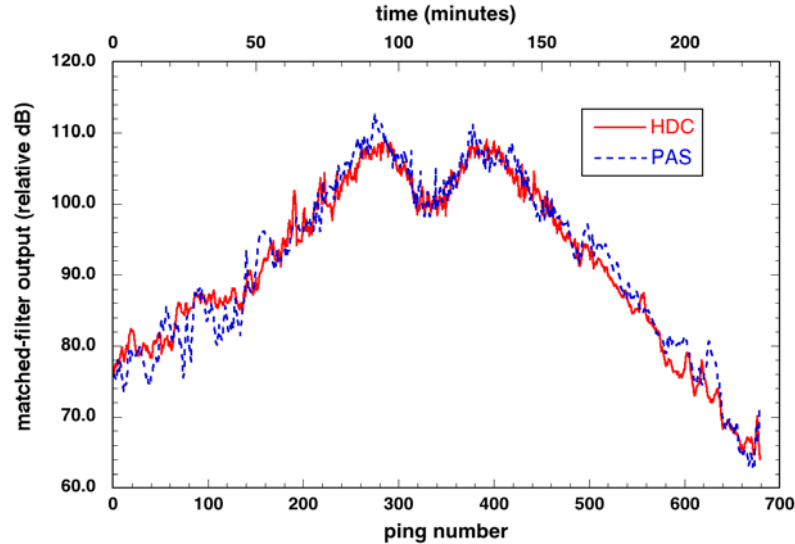
Fig. 3: Peak matched-filter output of each HDC and PAS ping. The minimum SRR for the run was 50 dB.

Fig. 4 shows the Doppler and time delay of the maximum amplitude arrival for each of the pings. The HDC and PAS Doppler follow the tactical Doppler (computed from the ship GPS) as expected. The large scale feature in the Doppler curves (from ping 250 to 450) occurs as the source passes through CPA, and back again, and the sign of the Doppler velocity changes. It may seem counterintuitive that the PAS Doppler fluctuations
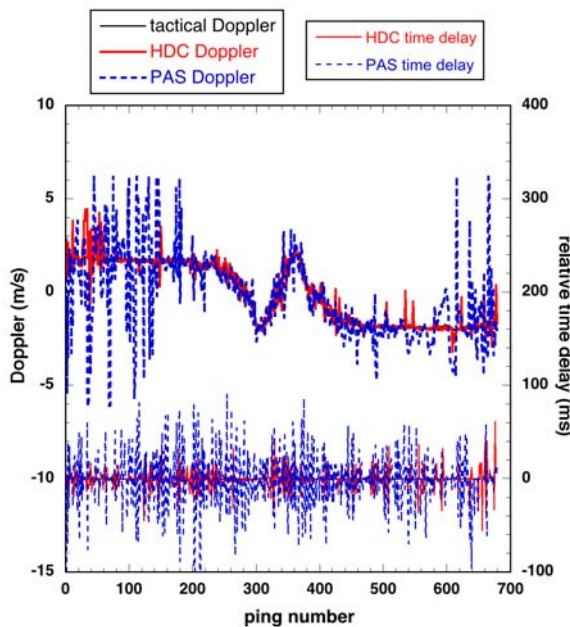

Fig. 4: Doppler (left scale and upper set of curves) and time delay (right scale lower set of curves) of peak arrivals. Tactical Doppler is the ship speed.
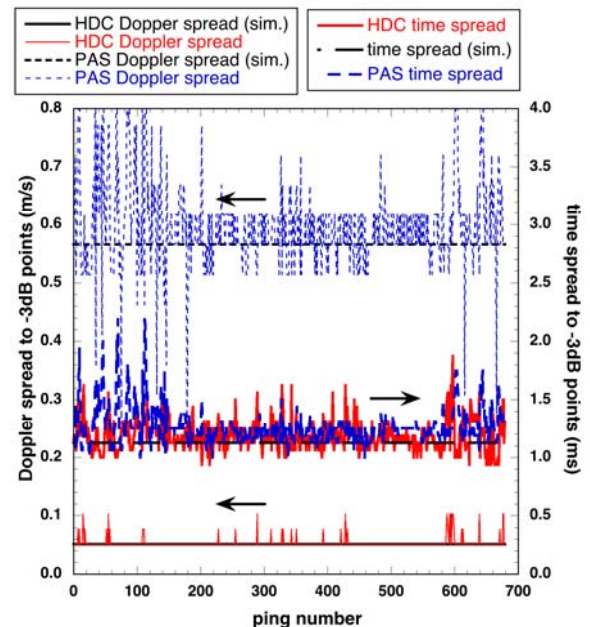

Fig. 5: Doppler spread (left scale) and time spread (right scale) of peak arrivals. The arrows point to the relevant axis for each group of curves.

are higher than for the HDC—especially evident at the start and end of the run. However, referring back to Table 1, one notes that the Doppler width is more than 3 m/s so there are only a few independent Doppler banks for the PAS pulse. This low Doppler sensitivity means that it only selects a different Doppler replica for large excursions from the tactical Doppler value. Put another way, the Doppler peak is so broad that even a small amount of noise on the signal could cause it to pick any of several replicas.

The HDC and PAS relative time delays were computed by measuring the ping-to-ping fluctuations in the arrival-time, relative to the pulse repetition time of 20 s, after correcting for the ping-to-ping range change. Fluctuations about the zero-delay line can occur because of fluctuations in the sound speed profile and/or the bathymetry, because amplitude fluctuations cause different multipath arrivals to be selected for different pings, or because the maximum arrival matches a Doppler bank that is different than the ship speed. Since the PAS pulse is much less sensitive to Doppler that the HDC pulse, it is probably this third effect that causes the greater fluctuations in the time delay that can be seen in PAS rather than in HDC.

Fig. 5 shows the two-sided Doppler and time spreading measured to the -3 dB down points for each ping of the run. Note that this is not a measure of the -3 dB down points in the wideband approximation mentioned earlier in the paper. That is a measure along the ridge of the AF defined in (5). The measurement here are the orthogonal transects along the Doppler and time axes. So rather than a measure of the ambiguity, it is a measure of the spreading in Doppler and time. The three horizontal black lines were computed from the zero Doppler, zero time-delay replica numerical simulations. The upper pair of curves (corresponding to the left vertical axis), show the measured and modelled PAS Doppler spread, and the lower pair (also corresponding to the left vertical axis) show the measured and modelled HDC Doppler spread. The middle set of three curves correspond to the right hand vertical axis and are the measured and modelled time spread for HDC and PAS. There is only one theoretical curve for the time spread since the AF time spread is determined by the bandwidth which is the same for HDC and PAS.
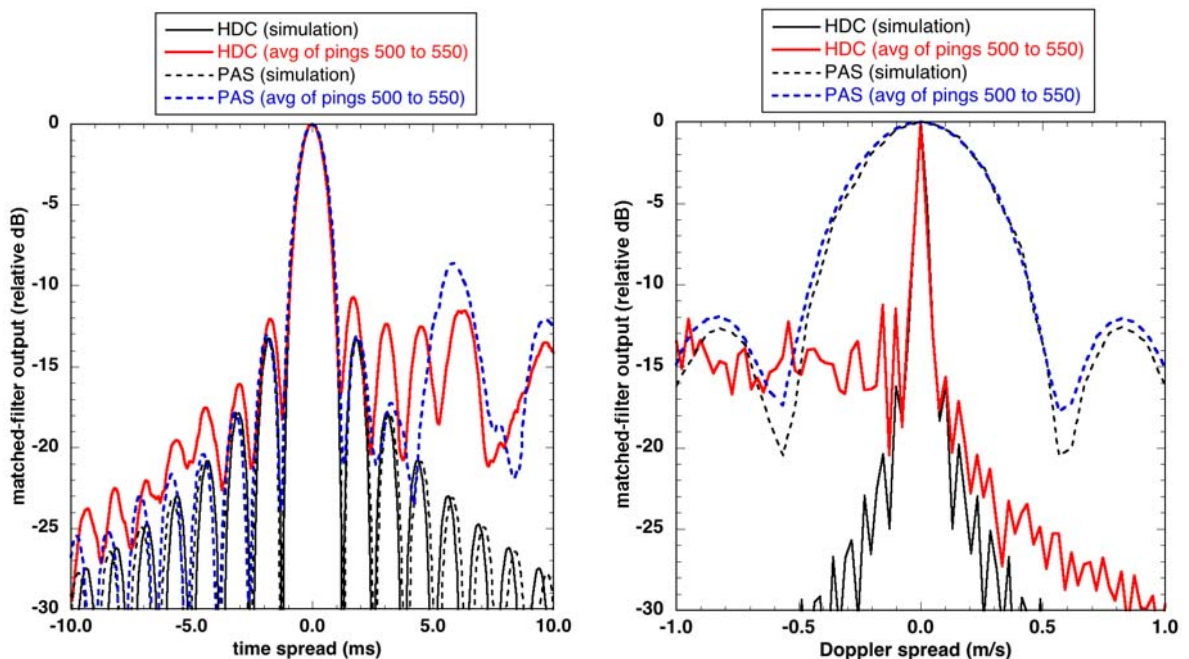

Fig. 6: Slice through zero range error (lhs) and zero Doppler (rhs). Black dashed lines are for PAS pulse parameters and solid red lines are for HDC pulse. Data are average of pings 500–550.

By plotting the orthogonal slices through the origin of the AF, one can compare the Doppler and time mismatch for the HDC and PAS. However, rather than using the theoretical curves, a numerical simulation was done using the HDC and PAS replicas. Doing this captures processing artifacts and pulse shading which will allow for a more accurate comparison with the experimental data. The simulation—which returned nearly identical results to the theoretical calculation—are shown in Fig. 6 as the solid black curves (HDC) and dashed black curves (PAS). These values were used for the modelled spreading estimates in Fig. 5 as well. Since time resolution for an LFM is proportional to $1/B$, both the HDC and PAS pulses have the same time resolution as shown in the *lhs* of the figure. In contrast, Doppler resolution is proportional to c/f_oT which results in much higher resolution (a narrower peak) for the HDC pulse shown in the *rhs*. The data in the plots are the average of pings 500–550 from a region in the data where the Doppler and time fluctuations are fairly low (recall Fig. 4). The agreement between the data and the numerical simulation indicates that there is very little environment-induced spreading. The asymmetry in the data around the peak is due to multipath interference.

We conclude the paper with an example of more substantial spreading seen by examining an individual HDC and PAS ping in Fig. 7. Insufficient analysis has been conducted thus far to comment on the specific cause of the spreading. It is presumed to be environmentally driven and is included to demonstrate that there is significant spreading in some of the data that merits further investigation. This will be the focus of future work.
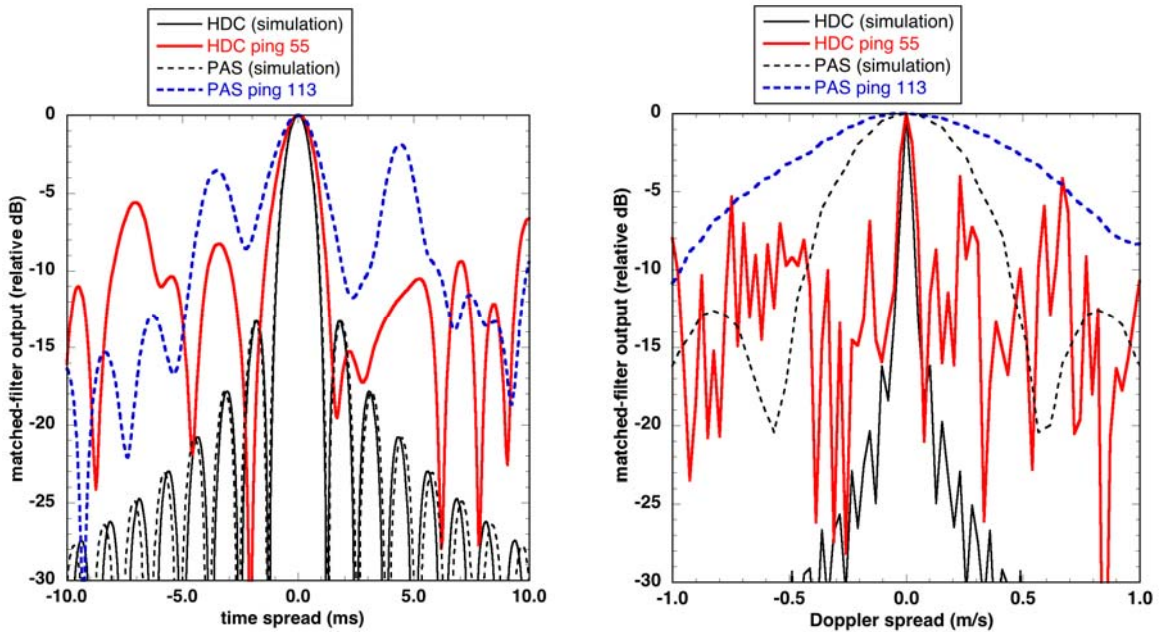

Fig. 7: Slice through zero range error (lhs) and zero Doppler (rhs). Black dashed lines are for PAS pulse parameters and solid red lines are for HDC pulse. Data are for a single ping.

5. ACKNOWLEDGEMENTS

Establishment (NOR), the Defence Technology Agency (NZL), and the Office of Naval Research (USA).

REFERENCES

[1] **Richard O. Nielsen**, *Sonar Signal Processing*, Artech House, 1991, p 204.
[2] **Stuart A. Kramer**, Doppler and Acceleration Tolerances of High-Gain, Wideband Linear FM Correlation Sonars," *IEEE Proceedings*, **55** (5), pp. 627-636, 1967.